ELSEVIER

Polymer 42 (2001) 8289–8295

polymer

www.elsevier.nl/locate/polymer

Effects of molecule aggregation state on dynamic mechanical properties of chlorinated polyethylene/hindered phenol blends

Chifei Wu*, Kazue Mori, Yoshio Otani, Norikazu Namiki, Hitoshi Emi

Department of Organic and Polymer Materials Chemistry, Faculty of Technology, Tokyo University of Agriculture and Technology, 2-24-16 Naka-cho, Koganei, Tokyo, 184-8588 Japan

Received 30 August 2000; accepted 8 February 2001

Abstract

The thermal properties of tetrakis [methylene-3-(3,5-di-*tert*-butyl-4-hydroxy phenyl) propionyloxy] methane (AO-60) and the dynamic mechanical properties of chlorinated polyethylene (CPE)/AO-60 hybrids were investigated. AO-60 is a crystalline material, but after heat-treatment AO-60 was found to possess two phases: a general amorphous phase and a highly ordered phase. A mixture of CPE and non-heat-treated AO-60 showed only one transition, whereas for a hybrid of CPE/AO-60 in which some of the AO-60 molecules had dissolved into the CPE matrix and most of the AO-60 molecules had formed glassy AO-60-rich domains, a new transition appeared above the glass transition temperature of CPE. This transition was thought to be due to the dissociation of intermolecular hydrogen bonds between CPE and AO-60, and the transition could be controlled by the thermal treatment, which caused a change in the aggregation state of the AO-60 molecules from amorphous to crystal state.

1. Introduction

In recent studies [1–4], we extensively investigated the dynamic mechanical properties and morphologies of CPE hybridized by hindered phenol compounds (HPC) such as 3,9-bis[1,1-dimethyl-2{β -(3-*tert*-butyl-4-hydroxy-5-methylphenyl)propionyloxy}ethyl]-2,4,8,10-tetraoxaspiro[5,5]-undecane (AO-80) and tetrakis [methylene-3-(3,5-di-*tert*-butyl-4-hydroxy phenyl)propionyloxy] methane (AO-60). It was found that a CPE/HPC blend, known as an organic hybrid, is a characteristic microphase-separated system in which there are two phases: a CPE-rich continuous phase and a HPC-rich domain. As a consequence of the HPC-rich domain, an additional transition above the glass-transition temperature of CPE was observed in the dynamic mechanical spectra and differential scanning calorimetry (DSC) curves. This discovery provides a new concept for controlling polymer material properties. The impact on the physical and mechanical properties of this novel transition can be formidable. The primary effect of functionalization of a polymer (or polymer blend) by the addition of HPC is enhancement of the damping properties because the tanδ peak of this novel transition is very high [1,5–7]. In addition, reversible hydrogen bonding, which acts as the tie points for the CPE-rich continuous phase, can lead to the discovery of shape memory function [1]. In those cases, control of this novel transition is important for modification of mechanical properties and for an understanding of the molecular mechanism.

The main results obtained from studies on the dynamic mechanical behavior of organic hybrids can be summarized as follows. The novel transition caused by the addition of HPC to CPE is attributed to the dissociation of intermolecular hydrogen bonds between the α-hydrogen of CPE and the hydroxyl groups of HPC in the HPC-rich domains. It was found that the intensity of this novel transition varies according to the number of intermolecular hydrogen bonds in the HPC-rich domains. On the other hand, it was found that the AO-60 molecules within the CPE matrix crystallize easily during an aging or heating process, and crystallization of AO-60 molecules results in the number of intermolecular hydrogen bonds between CPE and AO-60. Consequently, the novel transition can be controlled by heat-treatment below the melting point of AO-60.

The influence of heat-treatment temperature on the shapes of the AO-60 crystals was investigated in a previous study [8]. In this study, it was found that AO-60 crystals changed in sequence from monoclinic to lamella, needle, and finally imperfect crystal with decreases in the annealed temperature. In the present study, we focused on the amount of the AO-60 crystals when the AO-60 content

* Corresponding author. Tel.: +042-388-7225; fax: +042-381-7979.
E-mail address: wucf@cc.tuat.ac.jp (C. Wu).

0032-3861/01/$ - see front matter
PII: S0032-3861(01)00203-8

and heat-treatment temperature is invariable. Because in addition to the shape of the AO-60 crystal, that the amount also changed was a drawback in the previous study. The primary goal of the present study was to determine the relationship between the height of the tanδ peak and the aggregation state of AO-60 molecules within the CPE matrix. For this purpose, three kinds of CPE/AO-60 samples with different aggregation states of AO-60 molecules were prepared. We were particularly interested in trying to elucidate the structure of the AO-60 crystals.

2. Experimental

2.1. Materials

The CPE used in this study, which had a chlorination degree of 40 wt%, was of commercial grade (Daisolac RA140, Daiso Co.). CPE of this grade only crystallizes slightly, and its melting point is 105°C. The AO-60 (Fig. 1) used as a functional additive was a commercial antioxidant (ADK STAB AO-60, Asahi Denka Industries Co.). Its melting point is 116°C. However, AO-60 quenched into an ice-water bath from a temperature higher than its meting point is a glassy material. Moreover, if an isothermal crystallization or heat treatment is carried out, the crystalline AO-60 also becomes a glassy material, and its glass transition temperature is 44°C.

In this study, three kinds of CPE/AO-60 samples with different the aggregation states of AO-60 molecules were prepared. The CPE powder was kneaded by mixing rollers for 5 min, and then AO-60 crystal powder (Fig. 2) was added to the kneaded CPE. The AO-60 content was 40 wt% for all samples. The mixture was kneaded for 10 min at room temperature. The sample thus obtained, in which the AO-60 compound was dispersed into the CPE in the form of crystalline particles, is called sample A here. Moreover, the kneaded CPE/AO-60 mixture was made molten for 3 min and then pressed in a laboratory hot press at 160°C, which is higher than the melting point of AO-60, for 7 min under a pressure of 180 kg/cm^{-2}. The molten specimen was then rapidly quenched into an ice-water bath (sample B). The AO-60 molecules within the CPE matrix in sample B existed in the form of a glassy state. The quenched specimens were placed in a constant temperature chamber at 90°C for various times and then quenched into an ice-water bath. The resultant specimen, in which the AO-60 glass had partly crystallized, is called sample C. The AO-60 molecules in samples A, B and C were in the forms of crystal, glass, and a mixture of crystal and glass, respectively.

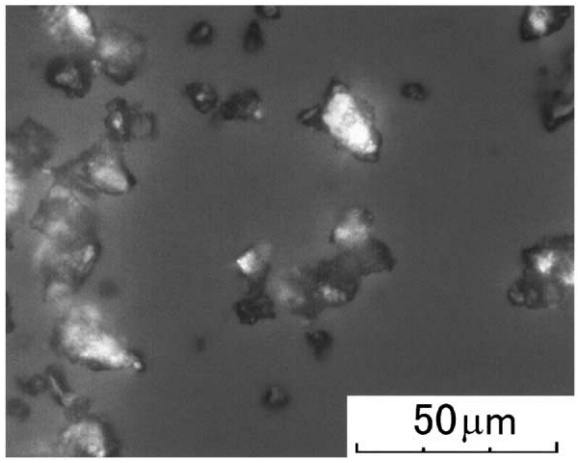

Fig. 2. Polarized light micrograph of AO-60 powders.

2.2. Dynamic mechanical analysis (DMA)

The dynamic viscoelastic measurements were made with a dynamic mechanical analyzer (DVE-V4; Rheology Co.), on sample specimens of the following dimensions; 20 mm long, 5 mm wide, and 1 mm thick. The temperature dependence of dynamic tensile moduli were measured between −30 and 100° at a constant frequency of 11 Hz and a heating rate of 3°C/min.

2.3. Differential scanning calorimetry (DSC)

DSC measurements were carried out with a Mettler Tredo calorimeter DSC820. Samples of about 20 mg in weight and sealed in aluminum were heated from −100 to 160°C at a scanning rate of 10°C/min under a nitrogen atmosphere in order to investigate melting temperature, degree of crystallinity, and glass transition temperature of AO-60, CPE and CPE/AO-60. The value of the glass transition temperature (T_g) was identified by extrapolated onset temperature of the transition region.

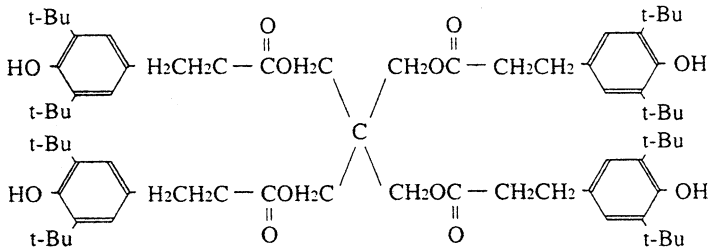

Fig. 1. Chemical structure of AO-60.

2.4. Optical microscopic observation

Samples placed between two cover glasses were observed under a polarizing microscope (OLYMPLS BX50) with a temperature controller (FP82HT) to examine the shape of crystals of pure AO-60 and AO-60 within the CPE matrix.

3. Results and discussion

DSC measurements were carried out to determine the thermal properties of pure AO-60. Fig. 3 shows DSC curves of untreatment AO-60 (1), quenched AO-60 (2), crystallized AO-60 (3) and annealed AO-60 (4). The untreated AO-60 was a crystalline material, while the other three samples were amorphous materials that clearly exhibited two second-order transitions, one at 44°C and one at 91°C. Therefore, quenched or heat-treated AO-60 is regarded as an organic glassy material. The first transition at 44°C is associated with the general glass transition, while the second transition at 91°C may be a phase transition from a true liquid state to a liquid that is fixed by hydrogen bonding between the hydroxyl groups of AO-60. The second transition is very different from the liquid–liquid transition [9], which has been observed in many amorphous and semi-crystalline polymers [10–14], and glass forming small molecules [9] in specific heat.

Fig. 4 shows the temperature dependence of the loss tangent (tanδ) for CPE and for CPE/AO-60 (samples A and B, respectively). In sample A, a slight decrease and shift in the tanδ peak due to the glass transition of CPE was observed. Another relatively low peak near the melting point of AO-60 also was observed. Those results imply that AO-60 is dispersed into the CPE matrix as crystalline particles. In contrast, sample B exhibited a novel peak above the glass transition temperature (T_g) of the CPE matrix. This suggests that sample B showed a phase separation, and the two peaks probably arise from the glass transition of the CPE phase and the AO-60 phase. The magnitudes of the two peaks, particularly that of the second peak, are remarkable. As seen in Fig. 4, the second peak is higher than the peak due to glass transition of pure CPE.

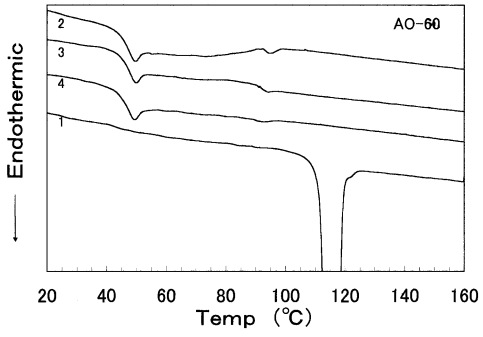

Fig. 3. DSC curves of various AO-60 samples: (1) untreated AO-60, (2) quenched in ice water, (3) isothermally crystallized at 90°C for 30 min, and (4) annealed at 90°C for 30 min. Scan rate was 10°C min^{-1}.

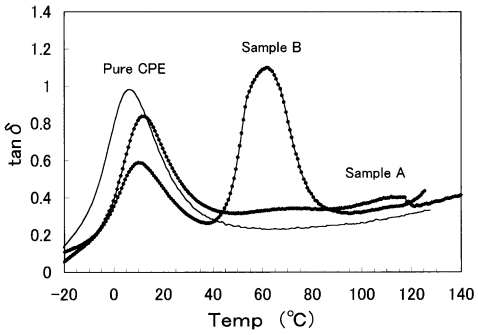

Fig. 4. Temperature dependence of loss tangent (tanδ) at 11 Hz for CPE and CPE/AO-60 (samples A and B).

Fig. 5 shows the temperature dependence of the storage modulus E' for samples A and B. Sample A exhibited a significant increase in the rubbery E' until the melting point of AO-60, exhibiting that AO-60 was dispersed into the CPE matrix as crystalline particles, because the AO-60 crystal particles only changed in size when CPE/AO-60 was kneaded below the melting point of AO-60. The increase in E' in the rubbery region can be interpreted as the addition effects of the inorganic fillers. On the other hand, the dramatic decrease in E' near 120°C is due to melting of the AO-60 crystals. By contrast, in the case of sample B produced by quenching sample A from 160 to 0°C, the E' curve clearly shows three dispersion regions in which E' changes rapidly with temperature (at 5, 60, and 115°C, respectively). The first dispersion centered at 5°C is associated with the glass transition of the CPE phase, while the second dispersion centered at 60°C reflects one transition of phase-separated AO-60 domains. This is different from the CPE/DZ system [15], in which there is only a glass transition. The E' in the intermediate plateau (20–45°C) for sample B is larger than that of pure CPE and sample A. The larger E' of sample B than that of sample A cannot be explained only in terms of the filled effects of fillers in the AO-60 domains, and it is thought that the phase-separated AO-60 domains of sample B have a peculiar structure. On the other hand, a shift of the first dispersion found from a comparison of sample B and pure CPE is also noteworthy. This is due to antiplasticizing effects of part of

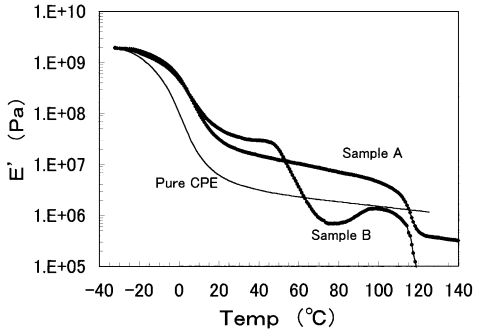

Fig. 5. Temperature dependence of storage modulus (E') at 11 Hz for CPE and CPE/AO-60 (samples A and B).

the AO-60 molecules dissolved into the CPE matrix phase. Therefore, sample B may be an incompletely phase-separated (in other words, partially compatible) system. Furthermore, the increase near 90°C and the decrease near 115°C in the E'-temperature curve may be due to the crystallization of AO-60 during the heating process and to the melting of the formed AO-60 crystal, respectively.

To clarify the origin of the novel transition, the aggregation state of the AO-60 molecules within the CPE matrix of sample B should be considered. Fig. 6 shows DSC curves of pure CPE and samples A and B. The CPE used is a slightly crystallized material. Sample A, being a blend of crystalline AO-60 and CPE, showed only a specific melting peak of the crystals of pure AO-60, indicating that AO-60 is dispersed into the CPE matrix as crystalline particles. In this case, a second transition was not observed. This implies that crystal particles of pure AO-60 cannot induce this novel transition.

In contrast, in the case of sample B, the melting peak of the AO-60 crystals was very small. That is, the crystallization of AO-60 molecules was suppressed by blending with CPE. This indicates that the AO-60 domain was almost an amorphous phase. The observed novel transition may be due to a transition of the glassy domain of pure AO-60 dispersed in the CPE matrix. That is, sample B is regarded as a completely phase-separated blend. If this were in fact the case, the second transition temperature would be close to the glass transition temperature of AO-60. As seen in Fig. 6, sample B also showed two transitions in the DSC curves. This trend agrees with the temperature dependence of tanδ (Fig. 4). This is different from some ionomers whose DSC thermograms show only one glass transition, corresponding to either that of the matrix or that of the cluster [16]. In order to confirm the origin of the second transition in the dynamic mechanical properties for sample B, we compared the second transition temperature of sample B with that of AO-60 in the DSC curves. It was found that while the two transition temperatures of pure AO-60 are 44 and 91°C, as seen in Fig. 3, the second transition temperature of sample B is 37°C, as seen in Fig. 6. Evidently, the supposition that the novel transition arises from glassy domain of pure AO-60 is highly unlikely.

It is reasonable to assume that the novel transition originates in a domain with peculiar structure in which the CPE segments are incorporated. Thus, a shift from 44 or 91°C to 37°C in the second transition temperature (DSC) can be considered to be a result of the incorporation of some CPE segments in the AO-60 domain. This assumption seems reasonable since the intermolecular hydrogen bond between α-hydrogen of CPE and hydroxyl groups of AO-60 is weaker than that between hydroxyl groups of AO-60 [2]. In addition, the incompletely separated phase-structure was confirmed by the existence of chlorine within the AO-60 domain [2].

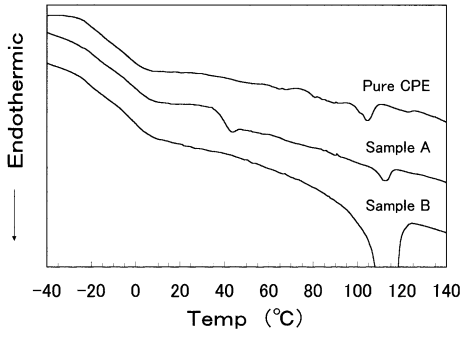

Fig. 6. DSC curves of CPE and CPE/AO-60 (samples A and B). Scan rate was 10°C min^{-1}.

Such an AO-60-rich domain can be considered to be a dynamic multifunctional cross-linking point. Thus, the observed additional plateau in the E'-temperature curve (Fig. 5) can be explained in terms of this cross-linking concept in addition to a filled filler concept. That is, the AO-60 domain included some CPE segments act not only as a filler but also as a cross-linking point. If the E' of the crystal particles of pure AO-60 is the same as that of the glassy AO-60-rich domains, the rise in E' from sample A to sample B can be attributed to cross-linking due to the AO-60-rich domains.

On the other hand, since the intermolecular hydrogen bonds between α-hydrogen of CPE and hydroxyl groups of AO-60 are dissociated above the second transition temperature, the AO-60-rich domain is released and therefore has no ability to behave as a junction point. As a result, E' dropped rapidly at around 60°C, as seen in Fig. 5. In this case, the AO-60 molecules act only as a plasticizer of CPE. The drop in E' at 75°C from pure CPE to sample B can be attributed to such plasticizing effects of the AO-60 molecules.

Since the second transition for sample B was attributed to the dissociation of intermolecular hydrogen bonds between CPE and AO-60 within AO-60-rich domains, the magnitude of the second transition would depend on the number of such intermolecular hydrogen bonds. In a recent related study [4], we analyzed the relationship between the height of the second tanδ peak and the content of AO-80, and we found that the second tanδ peak increases monotonously with increases in the AO-80 content and the number of intermolecular hydrogen bonds is therefore changed. In this study, we attempted to change the number of the intermolecular hydrogen bonds through annealing treatment. If the AO-60 molecules within the AO-60-rich domains crystallize, the CPE segments incorporated in the AO-60-rich domains may be eliminated during the crystallizing process. As a result, the second transition will become low due to the reduction in the number of intermolecular hydrogen bonds between CPE and AO-60.

On the other hand, the increase at temperatures above 80°C (until 95°C) in E' (Fig. 5) indicated that crystallization of AO-60 molecules within the CPE matrix is possible. It is therefore possible to change the number of intermolecular hydrogen bonds; this, of course, would to lead a lowering of the second transition.

Quenched specimens of CPE/AO-60 (sample B) were

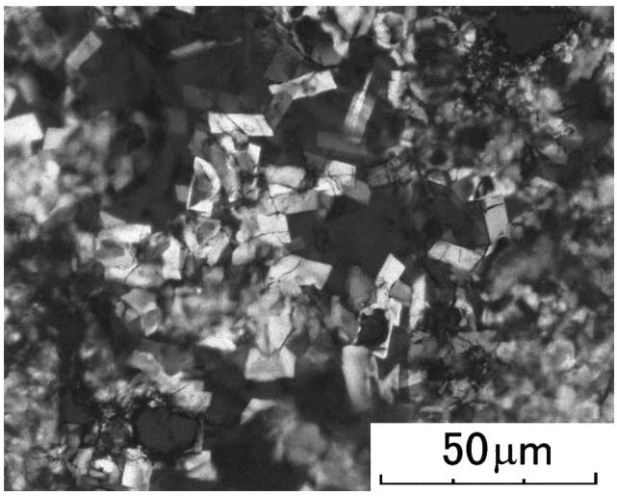

Fig. 7. Polarized light micrograph of AO-60 crystals in sample C90/30.

subjected to annealing temperature at 90°C. Fig. 7 shows a polarized optical micrograph of a sample annealed at 90°C for 30 min, denoted here as sample C90/30 (The numbers before and after the slanted line indicate annealing temperature and time, respectively.). Large lamella crystals of AO-60 were observed. The shapes and sizes of those crystals are very different from those of pure AO-60. This is due to the incorporation of CPE segments into the formed AO-60 crystals [8].

Fig. 8 shows the DSC curves of quenched sample B and various annealed samples C. For sample B, the melting peak due to the AO-60 crystals is very small, implying that most AO-60 molecules did not crystallize. With increases in annealing time (up to 8 min), the melting peak of AO-60 crystals increased. This is thought to be due to crystal growth from the AO-60-rich domain or the micro-crystal that fell into the disorder very much. With further increases in annealing time, there was almost no change in the magnitude of this peak from 16 to 45 min of annealing time, but another shoulder appeared near 100°C. This shoulder was probably caused by melting of an imperfect micro-crystal, which is thought to be a result of slight adjustment of the AO-60 molecules packed randomly in terms of position and

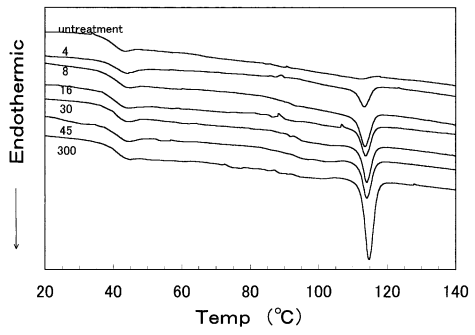

Fig. 8. DSC curves of CPE/AO-60 (samples B and C). Scan rate was 10°C min^{-1}. The numbers shown in the figure are annealing times (min).

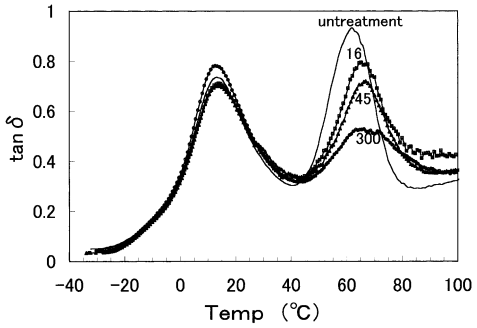

Fig. 9. Temperature dependence of loss tangent (tanδ) at 11 Hz for CPE/AO-60 (samples B and C). The numbers shown in the figure are annealing times (min).

direction as well as conformation in the AO-60-rich domain. The relatively low melting point is thought to be due to the disorder of the formed AO-60 crystals and/or of the incorporation of the CPE segment into the AO-60-rich domain. Furthermore, when the annealing time was extended to 300 min, the above-mentioned shoulder conversely became smaller, but the melting peak of AO-60 crystals, which appeared at 115°C, increased again. This suggests that there is a transition from an imperfect micro-crystal to a lamella crystal during an annealing process of more than 45 min. The result showed that the amount and regularity of the AO-60 crystals that formed during the annealing process varied greatly according to the annealing temperature. In summary, the process of 300 min annealing treatment can be classified into three regimes: (1) growth of micro-crystal, (2) formation of imperfect micro-crystal, and (3) transition from an imperfect micro-crystal to a lamella crystal.

Moreover, a comparison of the magnitude of the AO-60 melting peak of sample C (Fig. 8) and that of pure AO-60 showed that all annealed samples are partially crystalline. As for the sample as well whose annealing time is the longest, the amount of AO-60 crystals within the CPE matrix is less than that of pure AO-60. This suggests that crystals and amorphous material coexist in all annealed samples.

Fig. 9 shows the effects of annealing treatment at 90°C on

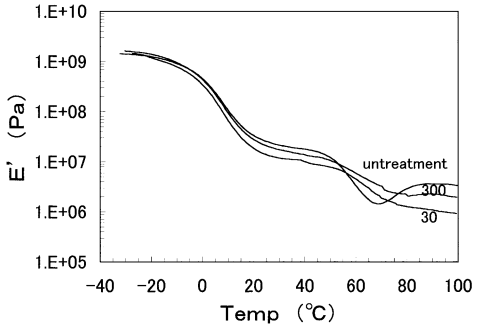

Fig. 10. Temperature dependence of storage modulus (E') at 11 Hz for CPE and CPE/AO-60 (samples B and C). The numbers shown in the figure are annealing times (min).

Table 1

	Sample A	Sample B	Sample C
Method for preparing sample	Mixing only	Mixing; pressing–quenching	Mixing; pressing–quenching; annealing–quenching
Aggregation state of AO-60 molecules	As a crystal particle	Incompletely phase-separated (partially compatible) (1) CPE-rich matrix phase (2) AO-60-rich domain	Incompletely phase-separated (partially compatible) (1) CPE-rich matrix phase (2) AO-60-rich domain (3) AO-60-rich crystal particle
Dynamic mechanical properties (second-order transition)	CPE's glass transition only	(1) CPE's glass transition	(1) CPE's glass transition
		(2) A novel transition (larger)	(2) A novel transition (smaller)

the temperature dependence of tanδ for samples B and C. There was no great change in the first peak with change in the annealing temperature, but the second peak decreases monotonously with increases in the annealing time. Considering that the second transition is associated with intermolecular hydrogen bonds between CPE and AO-60 within the AO-60-rich domain, the observed reduction in the second peak seems to be due to dissociation of the intermolecular hydrogen bonds during the crystallization process of AO-60 molecules due to annealing. The results demonstrated that the second transition caused by the dissociation of intermolecular hydrogen bonds was controlled through annealing treatment so that the number of the intermolecular hydrogen bond changes.

It is also noteworthy that there was almost no change in the position of the second peak for all samples, indicating that neither the annealing time nor temperature influences the second transition temperature. This implies that the second transition temperature depends on the intensity of the intermolecular hydrogen bonding but does not depend on the number of intermolecular hydrogen bonds, which is thought to determine the height of the second peak.

Fig. 10 shows the effects of annealing treatment at 90°C on the temperature dependence of E' for samples B and C. We focused on E' in the intermediate plateau (20–45°C), and we found that the influence of annealing treatment on E' is of particular interest. The E' of sample C90/30 annealed at 90°C for 30 min was lower than that of untreated sample B. When the AO-60 molecules within the AO-60-rich domains crystallize, the CPE segments incorporated into the AO-60-rich domains will be eliminated. Therefore, the drop observed in the intermediate regime of E' is thought to be a decrease in the crosslinking effect of the AO-60-rich domain as a dynamic crosslinking point. The E' of sample C90/300, which was subjected to longer annealing, was found to be larger than that of sample C90/30. If the modulus of the AO-60 crystal particles is larger than that of the amorphous AO-60 domain, this rise might be due to an increase in filler filled effect. However, as mentioned above, crystallization of AO-60 molecules in the CPE matrix can leads to a decrease in the crosslinking effect. Therefore, a speculation that the CPE segments incorporated into AO-60-rich domains are eliminated during the crystallization process of AO-60 molecules is inapplicable to this last crystallization process. It is conceivable that further elimination of CPE segments does not occur during the transition process from an imperfect micro-crystal to a lamella crystal.

4. Conclusions

The thermal properties of AO-60 and the dynamic mechanical properties of CPE/AO-60 were investigated. It was found that AO-60 is a crystalline material but that quenched and heat-treated AO-60 possesses two phases: a general amorphous phase and a highly ordered phase. In a mixture with CPE, most of the AO-60 molecules formed AO-60 domains. The dissociation of the intermolecular hydrogen bonds between CPE and AO-60 within AO-60-rich domains led to the appearance of a novel transition above the glass transition temperature of the matrix polymer CPE.

It was also found that the dynamic mechanical properties and microstructures of CPE/AO-60 could be controlled by annealing treatment. The annealing process at 90°C can be classified into three regimes: (1) growth of micro-crystals, (2) formation of imperfect micro-crystals, and (3) transition from an imperfect micro-crystal to a lamella crystal. While the second tanδ peak decreases monotonously with increases in annealing time, the E' in an intermediate plateau (20–45°C) decreases for the first 45 min of annealing and then increases again. Such an increase in the modulus during the last crystallizing process suggests that some CPE segments remained in the AO-60 crystals during the transition from an imperfect micro-crystal to a lamella crystal. The relationships between the aggregation state of AO-60 molecules and dynamic mechanical properties of CPE/AO-60 for the three samples used in this study are summarized in Table 1.

References

[1] Wu C, Yamagishi T, Nakamoto Y, Ishida S, Nitta K, Kubota S. J Polym Sci B: Polym Phys 2000;38:2285.

[2] Wu C, Yamagishi T, Nakamoto Y, Ishida S, Nitta K, Kubota S. J Polym Sci B: Polym Phys 2000;38:1496.
[3] Wu C, Yamagishi T, Nakamoto Y, Ishida S, Nitta K, Kubota S. J Polym Sci B: Polym Phys 2000;38:2943.
[4] Wu C, Yamagishi T, Nakamoto Y, Ishida S, Nitta K, Kubota S. Kobunshi ronbunshu 2000;57:294.
[5] Wu C. J Polym Sci B: Polym Phys 2001;39:23.
[6] Wu C. J Appl Polym Sci 2001;80:2468.
[7] Wu C, Otani Y, Namiki N, Emi H, Nitta K. Polym J 2001;33:322.
[8] Wu C, Nitta K. Kobunshi ronbunshu 2000;57:449.
[9] Murthy SSN. J Polym Sci B: Polym Phys 1993;31:475.
[10] Park D, Keszler B, Galiatstos V, Kennedy JP. J Appl Polym Sci 1997;66:901.
[11] Boyer RF. J Appl Polym Sci 1987;33:955.
[12] Gourari A, Bendaoud M, Lacabance C, Boyer RF. J Polym Sci: Polym Phys Ed 1985;23:889.
[13] Gilham JK. Polym Eng Sci 1979;19:749.
[14] Kumler PK, Machajewski GA, Fitzgerald JJ, Denny LR, Keinath SE, Boyer RF. Macromolecules 1987;20:1060.
[15] Wu C, Yamagishi T, Nakamoto Y, Ishida S, Nitta K, Kubota S. J Polym Sci B: Polym Phys 2000;38:1341.
[16] Kim JS, Wu G, Eisenberg A. Macromolecules 1994;27:814.